Earth Planet. Sci. Lett. 635 (2024) 118687

Contents lists available at ScienceDirect

Earth and Planetary Science Letters

journal homepage: www.elsevier.com/locate/epsl

The effect of weathering in runoff-to-groundwater partitioning in the Island of Hawai'i: Perspectives for landscape evolution

Alida Perez-Fodich [a,*], Louis A. Derry [b,c], Jean Marçais [d], M. Todd Walter [e]

[a] Department of Geology, University of Chile, Santiago, Chile
[b] Department of Earth and Atmospheric Sciences, Cornell University, Ithaca, NY, USA
[c] Université de Paris, Institut de Physique du Globe de Paris, CNRS, F-75005 Paris, France
[d] Irstea, Centre de Lyon-Villeurbanne, Lyon, France
[e] Department of Biological and Environmental Engineering, Cornell University, Ithaca, NY, USA

A B S T R A C T

We investigated how runoff-to-groundwater partitioning changes as a function of substrate age and degree of regolith development in the Island of Hawai'i, by modeling watershed-scale hydrodynamic properties for a series of volcanic catchments of different substrate age developed under different climates. In the younger catchments, rainfall infiltrates directly into the groundwater system and surface runoff is minimal, consisting of ephemeral streams flowing on the scale of hours to days. The older catchments show increasing surface runoff, with deeper incision and perennial discharge. We hypothesize that watershed-scale hydrodynamic properties change as a function of their weathering history—the convolution of time and climate: as surfaces age and become increasingly weathered, hydraulic conductivity is reduced, leading to increased runoff-to-recharge ratios. To test this relationship, we calculated both saturated hydraulic conductivity (k) and aquifer thickness (D) using recession flow analysis. We show that the average k in the younger catchments can be between 3 to 6 orders of magnitude larger than in older catchments, whereas modeled D increases with age. Ephemeral streams with zero baseflow at daily timescales cannot be evaluated using the same method. Instead, we calculated the recession constant for two contiguous catchments developed on young ash or lava deposits of different ages. Increasing bedrock age results in slower recession response in these ephemeral streams, which is consistent with decreasing hydraulic conductivity. Our results highlight the role of the weathering history in determining the evolution of watershed-scale hydrologic properties in volcanic catchments.

1. Introduction

When and where rivers form is a fundamental problem for the study of landscape evolution (Montgomery and Dietrich, 1988). Since the pioneering studies of Horton (Horton, 1933), runoff-to-groundwater partitioning has been recognized as a key factor for river incision and landscape evolution. Stream inception and development is important from a geomorphological perspective for understanding the response of the landscape, and surface and groundwater budgets under uncertain climate scenarios. Our current understanding of the Critical Zone (CZ) expands on this problem, as erosion rates, fluid residence times, and chemical weathering rates—which depend on climate, lithology and biota—control the architecture of the Earth's living skin (Riebe et al., 2017). The subsurface hydrodynamic structure of the CZ as a whole determines the fate of runoff-to-groundwater partitioning and ultimately the evolution of the landscape. Thus, an immediate question to ask is to what extent do any of these factors determine landscape evolution?

Pedogenesis and biogeochemical alteration of parent rocks in hydrologic basins have the potential to significantly transform water fluxes and catchment structure (Brantley et al., 2011; Rempe and Dietrich, 2014; Riebe et al., 2017). Although several factors (e.g., time, climate, vegetation, rock/mineral composition, tectonics) control the extent of weathering in the CZ, due to their relatively simplified geology, volcanic landscapes constitute an exceptional natural laboratory to understand the effects of chemical weathering on the long-term hydrological response shaping landscape evolution. Several studies have established a first-order relationship between hydrologic partitioning and bedrock age in volcanic basaltic catchments (e.g., Curtis et al., 2020; Luo et al., 2010; Mushiake et al., 1981; Schopka and Derry, 2012; Vittecoq et al., 2014). For example, runoff-to-groundwater partitioning both in the Cascades (Jefferson et al., 2006; Jefferson et al., 2010) and Japan (Yoshida and Troch, 2016) changes as a function of substrate age, as the proportion of groundwater recharge—or baseflow component in stream discharge—is greater in younger substrate age catchments. The studies argue that groundwater recharge is high due to the initial high permeability of basalts (e.g., Custodio, 2004; Sanchez-Murillo et al., 2015; Smith, 2004; Violette et al., 2014), and decreases as a function of

* Corresponding author.
E-mail address: aliperez@uchile.cl (A. Perez-Fodich).

https://doi.org/10.1016/j.epsl.2024.118687
Received 29 November 2023; Received in revised form 21 March 2024; Accepted 22 March 2024
Available online 6 April 2024

soil development resulting from weathering, which limits water infiltration to the groundwater system. This change in hydraulic properties has been observed at the pedon scale in both the Hawaiian and Galapagos archipelagos, where measured vertical hydraulic conductivity decreases as a function of soil development (Adelinet et al., 2008; Lohse and Dietrich, 2005), which can hinder groundwater recharge and increase lateral surface flow. The decreasing hydraulic conductivity in volcanic landscapes has been widely recognized (Custodio, 2004; Violette et al., 2014) and measured at young (Vittecoq et al., 2023) and old (Vittecoq et al., 2014) basaltic edifices. While the exact mechanisms through which weathering impacts hydrodynamic properties—that depend on rock and soil fabric, composition, and strength—of the surface remain uncertain, it appears that there is a strong relationship between time and drainage development on volcanic surfaces (e.g., Jefferson et al., 2010; Yoshida and Troch, 2016). Moreover, solute export fluxes in volcanic islands also evidence the change in hydrologic partitioning as a function of weathering, since groundwater solute export fluxes dominate the weathering budget in younger—incision free—volcanic catchments (Rad et al., 2007; Schopka and Derry, 2012). However, in older catchments with significant soil development, the subsurface contribution of weathering-derived solutes declined relative to solute exports in runoff (Schopka and Derry, 2012). It appears that substrate age influence on runoff-to-groundwater partitioning is a common feature in volcanic regions. However, establishing a direct relation between weathering and hydrologic partitioning is not straightforward, as soil and regolith development remains unconstrained in the aforementioned studies. Althoguh decreasing hydraulic conductivity with increasing substrate age has been measured along soil chronosequences (Adelinet et al., 2008; Lohse and Dietrich, 2005), it is hard to scale these discrete site-specific measurements to watershed-scale changes in hydrologic partitioning (Fortini et al., 2021). Based on these observations from different basaltic terrains, we seek to investigate the weathering-derived changes in watershed-scale hydrodynamic properties that control runoff to groundwater ratios.

Rainfall patterns in Hawai'i are strongly influenced by the prevailing trade winds and rain shadow effects (Fig. 1), and the windward side of the island (NE) receives significantly more precipitation than the leeward side. Older surfaces on the windward side display more dissection and channel development than the younger surfaces even at similar rainfall (e.g., Murphy et al., 2016; Schopka and Derry, 2012). On leeward slopes with low precipitation, regolith development is much less pronounced, and channel development is much more muted even on the older surfaces. Volcanic substrates can weather rapidly under humid conditions. In Hawai'i the depth and degree of development of weathered regolith depends on both age and climate (e.g., Chadwick et al., 2022; Goodfellow et al., 2014). The effect of rainfall shows a characteristic threshold near the point where time averaged precipitation exceeds evapo-transpiration. Sites with mean annual positive water

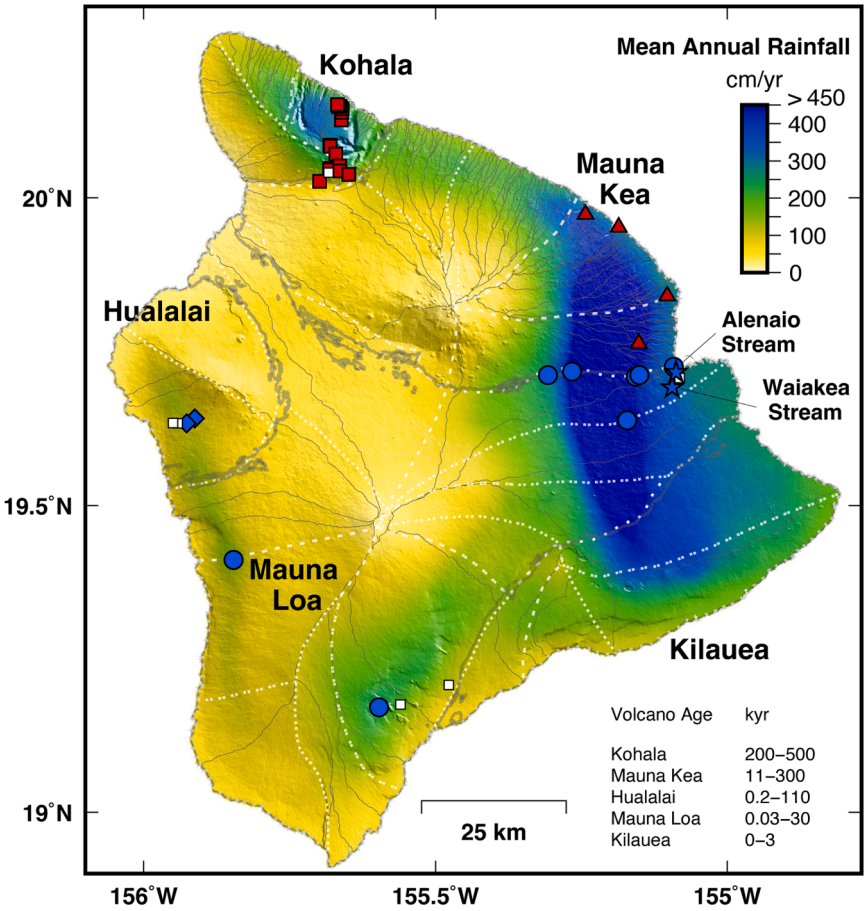

Fig. 1. Location of the stream gages for the studied streams. The blue symbols represent watersheds with a mean bedrock age < 30 kyr on eastern Mauna Loa (circles) and Hualalai (diamonds). The red symbols are watersheds with mean bedrock age > 30 kyr on Mauna Kea (triangles) and Kohala (squares). The blue star symbols are the ephemeral stream gage stations in the Hilo area. The white symbols are rain gage stations. The solid black lines represent the stream divisions based on the National Hydrography Dataset to the sub-watershed HUC12 scale. Dashed-white lines are the aquifer system divisions from Engott (2011). The color scale represents mean annual rainfall in cm. Rainfall data is from the Rainfall Atlas of Hawai'i project (Giambelluca et al., 2013). Elevation data are from the SRTM30 DEM (Becker et al., 2009). Gray solid lines are the limits between the different volcanic edifices for which area-weighted substrate age ranges are calculated based on the USGS Hawai'i Geologic Map (Sherrod et al., 2021; Wolfe and Morris, 1996).

balance show extensive soil development, while sites that have negative water balance show substantially less chemical depletion and thinner regolith (Bateman et al., 2019; Chadwick and Chorover, 2001; Chadwick et al., 2022; Chadwick et al., 2003; Perez-Fodich and Derry, 2019). While windward precipitation is variable, most windward area below the height of a regional inversion layer (ca. 1900 m), receive precipitation above this threshold. The area above the inversion contributes little to streamflow. Consequently, time is likely the main controlling variable for soil development. The trend of increasing channel density and dissection with age continues on the older islands across the archipelago (Schopka and Derry, 2012).

The observations documented above imply that the inception and development of stream drainage networks with permanent discharge on volcanic substrates is sensitive to their weathering history, and also allow to suggest an hypothesis: as the new volcanic surfaces are exposed to weathering and soils develop, water partitioning budgets change, direct infiltration and groundwater flow dominate in younger incision-free surfaces; whereas runoff-to-groundwater ratios increase on weathered surfaces with more developed stream networks. Thus, in this study we examine the recession behaviour to infer the hydrodynamic properties of volcanic watersheds of different bedrock ages and varying degrees of soil development. The hypothesis predicts that hydraulic conductivity at the watershed scale should be sensitive to the weathering history. As surfaces age and weather, hydraulic conductivity should decreases, with a resulting increase in runoff-to-groundwater ratios. To test this hypothesis, we estimate changes in the watershed-scale hydraulic conductivity across watersheds with different histories and degrees of regolith development. The initial meso-scale heterogeneity of porosity and permeability in volcanic terrains either from tephra or porous/fractured lava flows, and variable effects of the plant cover, makes it difficult for outcrop or pedon scale measurements to predict changes in runoff-to-groundwater partitioning at the watershed-scale (Allred and Allred, 1997; Fortini et al., 2021; Lau and Mink, 2006). Here, we use the method originally developed by Brutsaert and Nieber (1977) to model both hydraulic conductivity and aquifer thickness as watershed-scale parameters. The recession-based method is well-suited for our purposes, as it provides and estimate of watershed hydraulic parameters based on the overall response of the catchment to precipitation. Additionally, for two catchments with ephemeral streams—where the recession parameter estimation is impossible—we compare their stream runoff response through recession constant estimation, and correlate it to catchment bedrock age and soil development as proxies for thei weathering history. Finally, we then discuss a possible model of hydrologic evolution for the Island of Hawai'i.

2. Study area and methods

2.1. Water partitioning and regolith development across Hawai'i

Runoff-to-groundwater partitioning changes drastically across aquifer systems in the Island of Hawai'i based on the age of the volcanic surfaces, including lava flows and pyroclastic deposits, independently of rainfall (Figs. 1 and 2). We have grouped these aquifer systems in two categories considering their bedrock area weighted age resulting from their location in the different volcanic edifices—Kohala, Mauna Kea, Hualalai, Mauna Loa and Kilauea in descending age. As such, runoff-to-groundwater ratios are greater than 0.5 (with a mean Runoff/Recharge = 1.14) for all aquifer systems with mean bedrock ages > 30 kyr, with the exception of one aquifer system where rainfall is 50 cm/yr. In contrast, aquifer systems with mean bedrock ages < 30 kyr have runoff-to-groundwater ratios below 0.3 (mean Runoff/Recharge = 0.07) independent of rainfall, which ranges between 50–400 cm/yr according to Engott (2011) (Fig. 2(i)). It is important to note that at low mean annual precipitation (MAP) much of the water returns to the atmosphere as potential evapotranspiration (PET), and thus, runoff/recharge must be low when the water balance between MAP and PET is negative. In Hawai'i, MAP-PET > 0 occurs near 154 cm/yr of rainfall (Chadwick et al., 2022; Giambelluca et al., 2013), where excess water is available for either runoff or recharge. For the aquifer systems with MAP > 154 cm/yr there is a distinct threshold based on their mean bedrock ages. These exercise shows that runoff dominates in watersheds with older surface ages, whereas it makes up a small fraction of the water balance in younger watersheds, particularly those with mean bedrock age < 30 kyr (Fig. 2(ii)). In addition to the water balance, older surfaces such as those in Mauna Kea and Kohala host a significant number of streams compared to younger volcanoes in the island, as shown by the sub-watershed divisions (National Hydrology Database (NHD) HUC 12) in Fig. 1. The high density of stream networks in both Kohala and Mauna Kea is also evidenced by the difference in watershed areas when compared to younger catchments in Mauna Loa, Hualalai and Kilauea. Because of limited incision and the fact that subsurface flow may not reflect surface topography, watershed areas on the young surfaces are harder to define. Nevertheless, these younger streams have topographically delineated watershed areas 1–2 orders of magnitude greater those in Kohala and Mauna Kea (Tables 1 and S1). By examining the ephemeral or perennial flow regime for each individual catchment it is also possible to establish

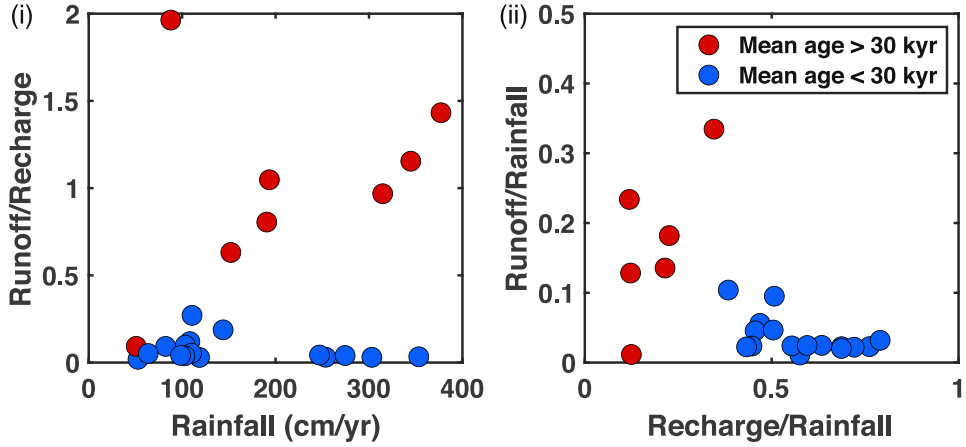

Fig. 2. Water balance for major aquifer systems in the Island of Hawai'i based on Engott (2011) and the State of Hawai'i Water Resource Protection Plan. The blue symbols represent aquifer systems with a mean bedrock age < 30 kyr on East Mauna Loa and Hualalai. The red symbols correspond to aquifer systems of mean bedrock age > 30 kyr on both Mauna Kea and Kohala. (i) Runoff-to-recharge ratio as a function of rainfall (cm/yr). The runoff-to-recharge ratio in aquifer systems with mean bedrock ages < 30 kyr is less than 0.5 at any rainfall. Only one aquifer system with mean bedrock age > 30 kyr has a ratio < 0.5. (ii) Rainfall normalized runoff versus rainfall normalized recharge. This relation highlights that recharge (when compared to runoff) dominates the water budget with mean ages < 30 kyr.

Table 1
List of stream stream gage stations for recession flow analyses. These stations have daily discharge records in the Island of Hawai'i, including watershed properties and area weighted geologic characteristics. All stream discharge data were obtained from the USGS National Water Information System (NWIS). Watershed properties including Basin Area, Longest Flow Path (LFP) and Probability of Zero Flows ($P(Q = 0)$) were obtained directly from the USGS database at the *StreamStats* application website and are updated through September 2022. The Recession Stream Analysis uses discharge data from all available records longer than 5 years through May 2019. Watershed area-weighted hydraulic conductivity (K_{sat}) was obtained from the USDA Web Soil Survey database utilizing the watershed delineated contours from StreamStats for each station. Similarly, the mean area-weighted substrate age for each watershed was calculated from the USGS Hawai'i Geologic Map (Sherrod et al., 2021; Wolfe and Morris, 1996). Mean Annual Precipitation was obtained for each station using the Hawai'i Rainfall Atlas online application (Giambelluca et al., 2013).

N	USGS Gage ID	Name	Lon	Lat	Area (km^2)	LFP (km)	MAP (cm)	P (Q=0)	K_{sat} (μm/s)	Mean Age (kyr)	Volcano	Start of Record	Last Record
1	16700000	Waiakea Stream	-155.172	19.639	49.4	32.5	339	0.004	82.29	2.2	E Mauna Loa	1930/10/01	1995/11/30
2	16701750	Wailuku River nr Humuula	-155.307	19.712	78.6	25	185	0.035	200.06	42.9	E Mauna Loa	1965/02/01	1972/09/30
3	16701800	Wailuku River nr Kaumana	-155.266	19.718	99.5	30.4	216	0.016	160.43	39.5	E Mauna Loa	1966/10/01	1982/09/30
4	16703000	Wailuku River at Pukamaui	-155.157	19.709	510	27.8	208	0.033	300.46	23	E Mauna Loa	1923/04/25	1940/05/24
5	16704000	Wailuku River at Piihonua	-155.151	19.713	571	65.4	236	0	285.96	30.9	E Mauna Loa	1928/07/01	2016/08/18
6	16713000	Wailuku River at Hilo	-155.092	19.726	636	72.8	259	0	280.46	31.3	E Mauna Loa	1977/03/01	1995/09/30
7	16717000	Honolii Stream	-155.152	19.764	31.2	21.9	477	0	7.3	61.5	SE Mauna Kea	1911/06/01	2016/08/18
8	16717600	Alia Stream	-155.103	19.841	1.7	6.5	483	0	3.41	182	SE Mauna Kea	1962/05/01	1972/05/31
9	16717800	Pohakupuka Stream	-155.186	19.953	7.3	16.2	413	0	4.18	98.2	NE Mauna Kea	1962/05/01	1979/11/09
10	16717820	Manowaiopae Stream	-155.243	19.973	2.7	3.8	417	0	3.34	113	NE Mauna Kea	1965/09/01	1971/10/12
11	16720000	Kawainui Stream	-155.68	20.085	4	4.5	421	0	26.18	376	S Kohala	1964/01/01	2016/08/18
12	16720300	Kawaiki Stream	-155.68	20.084	1.1	2.7	407	0.003	25.9	190	S Kohala	1968/06/01	1999/10/19
13	16725000	Alakahi Stream	-155.671	20.071	2.2	3.6	369	0.003	26.68	197	S Kohala	1964/01/01	2016/08/18
14	16737000	Waiilikahi Stream	-155.661	20.126	2	5.6	402	0	13.91	380	NE Kohala	1939/04/01	1959/12/31
15	16738000	Kaimu Stream	-155.661	20.139	2.1	6.6	343	0	7.73	380	NE Kohala	1939/04/01	1952/06/30
16	16739000	Punalulu Stream	-155.66	20.144	1.8	6.1	349	0	7.08	380	NE Kohala	1939/04/01	1952/06/30
17	16740000	Waiaalala Stream	-155.663	20.148	0.4	1.6	258	0	7.8	380	NE Kohala	1939/04/01	1952/07/31
18	16741000	Paopao Stream	-155.666	20.148	0.9	3.2	300	0	7.8	380	NE Kohala	1939/03/01	1952/09/30
19	16742000	Kukui Stream	-155.668	20.151	0.5	2.8	278	0	8.47	380	NE Kohala	1939/03/01	1966/09/30
20	16756000	Kohakohau Stream nr Kamuela	-155.68	20.047	6.2	8.1	263	0	18.45	250	S Kohala	1956/04/01	1966/12/06
21	16756100	Kohakohau Stream above intake	-155.681	20.046	6.4	8.5	260	0.012	18.29	250	S Kohala	1998/06/26	2011/12/04
22	16756500	Keanuiomano Stream	-155.699	20.027	11.5	12.4	207	0.084	24.31	190	S Kohala	1963/11/01	1972/09/15
23	16757000	Waikoloa Stream nr Kamuela	-155.664	20.052	2.3	3.7	261	0	22.37	190	S Kohala	1947/06/01	1971/09/30
24	16758000	Waikoloa Stream at Marine Dam	-155.663	20.044	3.6	4.9	233	0	12.19	190	S Kohala	1947/06/01	2011/12/06
25	16759000	Hauani Gulch	-155.649	20.038	1.2	2.5	180	0.025	100.77	20.5	SW Hualalai	1956/03/01	2004/10/03
26	16759200	Waiaha Stream nr Holualoa	-155.913	19.642	7.3	8.7	80	0.304	131.3	13.6	SW Hualalai	1960/05/01	1982/09/30
27	16759300	Waiaha Stream at Luawai	-155.926	19.634	21.6	14.6	78	0.404	121.3	13.6	SW Hualalai	1960/05/01	1971/09/30
28	16759800	Kiilae Stream	-155.846	19.411	2.8	8.4	111	0.39	254	2.4	W Mauna Loa	1958/05/01	1982/09/29
29	16764000	Hilea Gulch tributary	-155.597	19.171	4.4	6.4	175	0.164	10.21	38.8	SW Mauna Loa	1966/02/01	1991/09/30

differences between older substrate age (> 30 kyr) and younger catchments (Fig. 3(i), Tables 1 and S1): most catchments with substrate age > 30 kyr have a null probability ($P = 0$) of zero baseflow (with exception of the Wailuku); on the other hand, catchments with subtrate ages < 30 kyr are ephemeral streams with non-null probabilities ($P > 0$) of no baseflow in the water year despite their differences in MAP.

In addition to the water budget, we assessed soil development using in-situ saturated hydraulic conductivity (K_{sat} μm/s) estimates from the USDA Soil Survey dataset for the Island of Hawai'i (Fig. 3(ii)). This dataset is derived from the USDA soil hydraulic conductivity model based on soil characteristics observed in the field, which includes porosity, structure and texture. Thus, these values were derived as area-

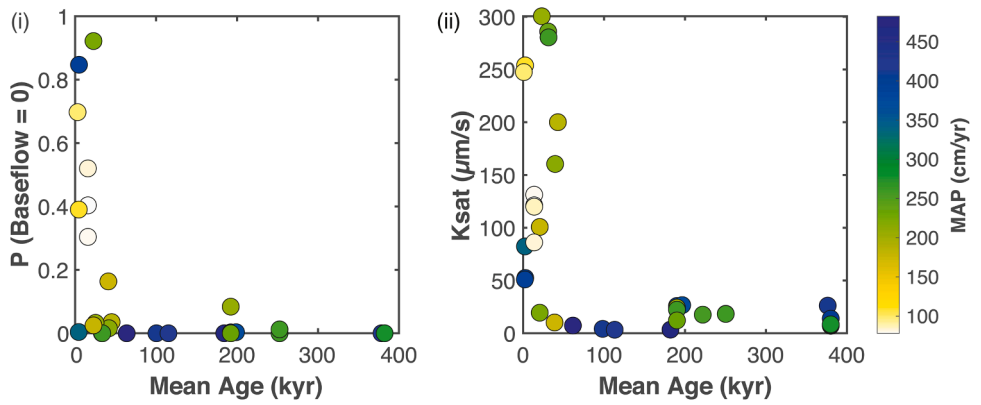

Fig. 3. Perennial discharge and soil derived hydraulic conductivity as a function of substrate age and mean annual precipitation. (i) Probability of baseflow = zero as a function of substrate area weighted age in kyr for the streams listed in Tables 1 and S1. The color scale represents the mean annual precipitation (MAP) in cm/yr where darker (blue) represents increasing precipitation rates. $P = 0$ indicates a perennial discharge, whereas $0 < P < 1$ is an intermittent stream. The probability of zero baseflow (P) is derived from Izuka et al. (2018). (ii) Saturated soil hydraulic conductivity (K_{sat}) averaged across soil types present in each stream drainage area as a function of age (kyr) and MAP (cm/yr). Hydraulic conductivity data from the USDA Web Soil Survey.

weighted averages from the soil series mapped within each watershed area. Fig. 3(ii) shows that hydraulic conductivity ranges across the different watersheds in the Island of Hawai'i according to their bedrock age, where the same threshold behavior observed for the water budget can be observed. K_{sat} ranges between 10 to 300 μm/s for watersheds with mean bedrock ages < 30 kyr, with a mean of 143 μm/s. Watersheds with mean bedrock ages older than 30 kyr in Kohala and Mauna Kea show field ksat values with a mean of 40 μm/s, ranging between 3–200 μm/s. Only the Wailuku watershed areas (USGS 16704000 and 16713000) with bedrock age >30 kyr have K_{sat} values greater than 20 μm/s). We note the Wailuku stream follows the contact between younger Mauna Loa and older Mauna Kea lavas along much of it length, and this represents a hybrid case. Field-based K_{sat} does not show any clear relation with respect to climate, both globally and when analyzing both bedrock age groups. Based on the water budget, the recession behavior—as probability of zero baseflow—, and the soil properties we can infer a relation with bedrock age, and thus, integrated weathering exposure that modulates catchment-scale hydrologic partitioning. From the observed relations between watershed area-weighted bedrock age, probability of zero baseflow, and water budget, from this point forward we group the watersheds in these two categories: (1) mean bedrock age < 30 kyr, and mean bedrock age > 30 kyr.

2.2. Recession flow analysis

Subsurface hydrology can be characterized in terms of saturated hydraulic conductivity (k), effective aquifer thickness (D) and specific yield (f) (Mendoza et al., 2003). These properties can be hard to estimate at the catchment scale if data from subsurface wells are scarce or unavailable (Huang and Yeh, 2019; Mendoza et al., 2003). However, even when data from well-tests are available (Rotzoll and El-Kadi, 2008), these constitute discrete values that cannot be extrapolated with confidence to whole watershed without additional information. Streamflow recession flow analysis (RFA) can provide quantitative information about watershed-wide hydrodynamic properties and can be complementary to discrete well-tests. The method developed by Brutsaert and Nieber (1977) can regionalize these hydrodynamic properties watersheds draining on unconfined aquifers, and several studies have used this method for different purposes—e.g., analyzing flow recession behavior or to directly calculate watershed-transmissivity (Brutsaert and Lopez, 1998; Huang and Yeh, 2019; Malvicini et al., 2005; Mendoza et al., 2003; Oyarzun et al., 2014; Sanchez-Murillo et al., 2015; Troch et al., 1993; Vannier et al., 2014; Vogel and Kroll, 1992; Zecharias and Brutsaert, 1988). Here, we use this method to calculate basin-wide effective hydrodynamic parameters: hydraulic conductivity and aquifer thickness, using daily discharge data from streams in Hawai'i. The approach provides a straightforward analytical method that we can apply to compare characteristics across multiple watersheds and requires minimal parameter estimation. The Brutsaert and Nieber (1977) method is based on the solution to the Boussinesq equation (Boussinesq, 1877) for drainage from unconfined rectangular aquifer (Eq. 1), where a and b are the recession constants, and a is related to basin-wide hydrodynamic parameters. Note that this representation approximates water draining at a certain rate from an aquifer which is proportional to the storage.

$$\frac{dQ}{dt} = -aQ^b \tag{1}$$

Eq. 1 describes the change of groundwater outflow (as baseflow) draining into a stream, and assumes streamflow is divided in two components that operate at short and long timescales. The short timescale behavior will follow a major precipitation event that recharges the aquifer, characterized by $b = 3$. The long-term behavior corresponds to recession flow with $b = 1.5$ (Brutsaert and Nieber, 1977) or b = 1 (Brutsaert and Lopez, 1998; Malvicini et al., 2005). Parlange et al. (2001) derived the analytical solution to both flow components. This analytical solution locates the transition point between these two regimes for a dimensionless flow at log (Q^*) = −0.1965 and log ($|dQ^*/dt|$) = 0.0918.

$$Q^* = \frac{A}{4l^2D^2k}\,Q \tag{2}$$

$$t^* = \frac{4l^2Dk}{fA^2}\,t \tag{3}$$

where k is the saturated hydraulic conductivity [LT^{-1}], D is the aquifer thickness [L], A is the watershed area [L^2], l the length of the stream [L] (l here as LFP), and f is the specific yield as volume fraction (Parlange et al., 2001). In Eqs. (2) and (3), f, D and k are unknown; thus, one of these parameters must be independently estimated. The translation vector (H, V) between the theoretical and the streamflow data transition points is used to estimate the watershed hydrodynamic parameters.

$$H = \frac{4l^2D^2k}{A} \tag{4}$$

$$V = \frac{16l^4D^3k^2}{fA^3} \tag{5}$$

We performed recession flow analysis using long-term daily stream discharge data on 22 perennial catchments monitored through 29

stream gages in Hawai'i draining volcanic deposits of different ages (Fig. 1, Table 1). The studied watersheds are located across the Kohala, Mauna Kea, Hualalai and Mauna Loa volcanoes, which are later grouped according to their mean area-weighted substrate age (cutoff at 30 kyr). Watershed area, longest flow path (LPF), MAP and substrate age for the oldest watersheds in Kohala and Mauna Kea range between 0.5–31 km^2, 2.7–22 km, 207–483 cm/yr, and 62–380 kyr. For Hualalai, area ranges from 1.2–21.6 km^2, LPF within 2.5–15 km, MAP at 78–180 cm/yr, and ages between 14–21 kyr. Eastern Mauna Loa watersheds have areas within 50–636 km^2, LFP from 25–73 km, MAP from 185–339 cm/yr, and ages at 2–43 kyr. The two western Mauna Loa watersheds have a mean area of 3.6 km^2, mean LFP of 7.4 km, MAP of 143 cm/yr, and 20.6 kyr. All discharge records are longer than 5 years with varying starting and ending dates (Table 1). Details are available on the Data Sources and Methods section in the Supplementary Information, where we describe the strategies used for data selection and filtering for baseflow and slow recession behavior. After the daily discharge data is filtered, the analysis requires locating the transition point (Eqs. 4 and 5), which is not obvious from the data. Therefore, we use three different models to locate the transition point based on the strategy implemented by (Mendoza et al., 2003). Details can be found in the SI. Potential biases or uncertainties in the estimated k and D parameters stem first from the choice of model to locate the position of the transition point between low and high flows, and secondly from the uncertainty in the specific yield f. We discuss these biases in a later section.

Finally, we examine the response to rainfall events of two contiguous ephemeral streams of different substrate age located on Mauna Loa (Fig. 4) by comparing their recession constants. For this analysis we used instantaneous (15-minute) discharge data (Supplementary Information and Table S2).

3. Results and discussion

3.1. Estimation of watershed scale hydrodynamic parameters

We calculated both hydraulic conductivity k and aquifer thickness D for each perennial stream (Table S3) based on the placement of the three transition points from the recession flow analysis (Figs. 5, S1 through S5). For our analyses, we tested the value of the specific yield f from a wide range of published values for basalts and other types of rocks (Wolff, 1982), and selected values of f on the lower end of available data (10^{-7} to 10^{-5}). We selected this range of specific yield values based on the preliminary assessment of the method for a larger range of f. A value of $f > 10^{-5}$ results in aquifer thickness $D \leq 1$ (mm), which implies the absence of a groundwater supply to baseflow. For the results presented here, we assumed a specific yield $f = 10^{-6}$, resulting in hydraulic conductivities between $10^{-6} < k < 10^{2}$ (m/s), and aquifer thickness between $10^{-2} < D < 10^{2}$ (m). Although the hydraulic conductivity values are only approximate estimates based on the recession flow analysis and its inherent uncertainties, these values are within the range of previously modeled and measured borehole pumping tests in Hawai'i (Ingebritsen and Scholl, 1993; Izuka, 2011; Rotzoll and El-Kadi, 2008), and also those from pumping tests in volcanic islands like Mayotte (Vittecoq et al., 2014) and Martinique (Vittecoq et al., 2023). Note also that Eqs. (4) and (5) imply that larger specific yield values—closer to the upper boundary reported for basalts ~ 0.1 (Deolankar, 1980; Singhal and Gupta, 2010)— would result in unrealistically small aquifer thickness D, in the order of ~ 10^{-5} meters, and will predict $k \gg 1$ (m/s).

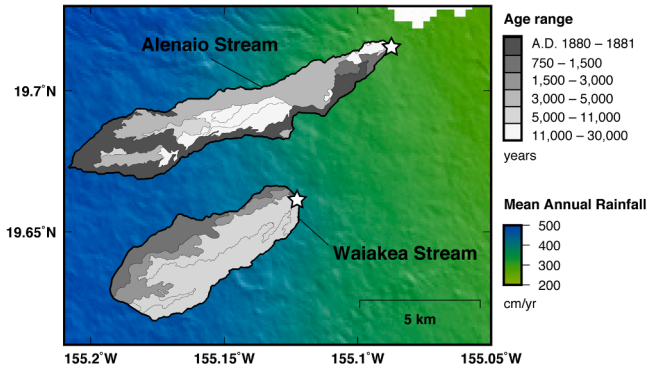

Fig. 4. Substrate age units represented for the Alenaio and Waiakea watersheds. The dark-to-light grading shades of gray represent the increasing age ranges based on the mapped units. The stars show the stream gage location for the analyzed data. The units are overlying the interpolated mean annual rainfall map from Fig. 1. Note that the watershed limit for the Waiakea stream was modified to only contain the portion with mapped surface runoff according to the USGS topographic database. This map was created using the GIS database from the USGS (Sherrod et al., 2021).

Based on the watershed substrate age categorization—which is also related to the ephemeral or perennial character of the streams, or more specifically, the probability of zero flows (Table 1)—we could not make a distinction between the Kohala and Mauna Kea groups in terms of their estimated k and D values This is consistent with their overall similar degrees of weathering and pedogenesis (Fig. 3(ii)) (Chadwick et al., 1999; Vitousek, 2004; Vitousek et al., 1997). However, the modeled aquifer thickness for the Mauna Loa watersheds is greater than for the Hualalai watersheds located on the lee side of the island. This is also consistent with higher MAP that results in higher baseflow indexes in Mauna Loa compared to the catchments in Hualalai.

3.1.1. Uncertainties in hydrodynamic parameters

The largest uncertainties in the estimated parameters derive from the choice of strategy to locate the transition point. Each method for locating the transition point yields results for k that can differ by a factor of 1–100 depending on the watershed, with root-mean-square deviations between 0.15–0.75 between the logarithm of the estimated parameters by the different models (Fig. S6). The estimates obtained from TP1 and TP2 are well correlated (with $R^2 = 0.992$) and show very small deviations. On the other hand, placement of the third transition (TP3) point shows more variation with respect to modeled k and D in TP1 and TP2, as the correlation coefficients are < 0.8 and the deviation between models is larger (Figure S6). However, in all cases the three transition points allow separation of k and D for the watershed groups according to their substrate age (Fig. 5). Thus, regardless of the placement of the transition point, the recession flow analysis yields comparable results that allow to distinguish the differences in both hydraulic conductivity and aquifer thickness based on the substrate age and the weathering history for the watersheds in Hawai'i.

Although we provide three different models for the location of the transition point, these models also rely on the precision of the data which define the lower and upper envelopes in the $\log(|dQ/dt|)$ vs $\log(Q)$ space which is determined by the time-step (Δt) for calculating the derivative of discharge. Specifically, Rupp and Selker (2006) demonstrate that a fixed time-step—usually given by the gage precision—for calculating dQ/dt at high and low flows might be not sensible at low flows. We did not attempt to calculate a variable time-step in our study. Such an exercise would require either: 1) evaluating sub-daily Δt for the high flows to capture the highest rates of decline in discharge, which could allow to identify the transition point closer to TP3—but this is impossible because we use daily-records; or 2) using a longer time-step for the low flows to decrease the noise introduced by the discharge derivative, with a transition point in the vicinity of TP1 to TP2 (Figs. S2-S5 and S6) (e.g., Kirchner, 2009; Roques et al., 2017; Rupp and Selker, 2006).

In addition to the inherent uncertainty in the modeled parameters, for our analysis (Eqs. (4) and (5)) we had to fix one of the unknown hydrodynamic parameters (specific yield f) to calculate the rest. We also assume that the fixed parameter f is constant and thus, hydraulic conductivity (k) and aquifer thickness (D) are constant too. Although we

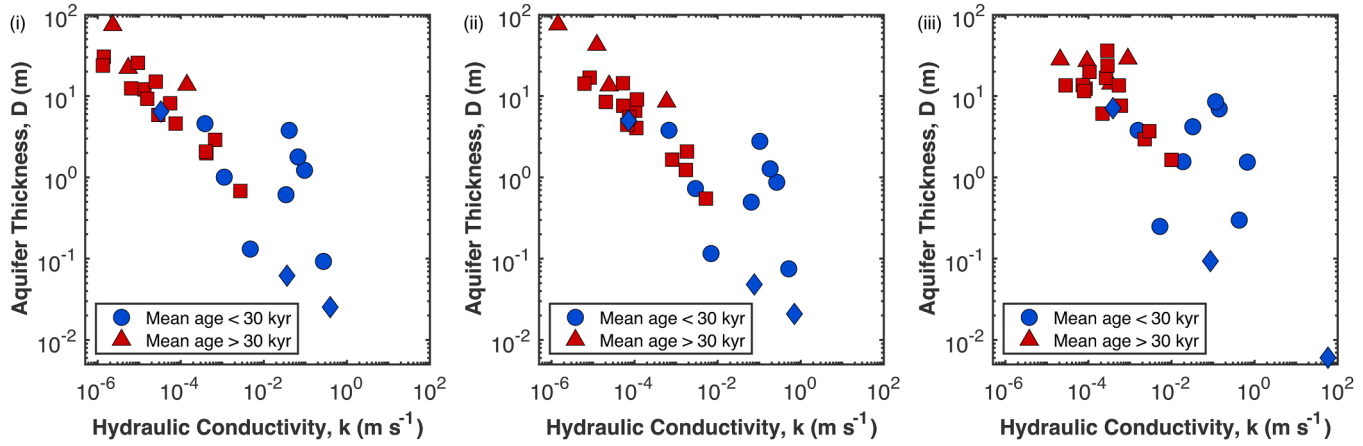

Fig. 5. Calculated hydraulic conductivity and aquifer thickness from recession flow analysis at specific yield $f = 10^{-6}$ for the three recession points at (i), (ii) and (iii) respectively. The blue symbols represent watersheds with a mean bedrock age < 30 kyr on Mauna Loa (circles) and Hualalai (diamonds). The red symbols correspond to watersheds of mean bedrock age > 30 kyr on both Mauna Kea (triangles) and Kohala (squares).

cannot independently measure or estimate the specific yield (f), there are a few considerations that allow us to assess a range of values for f. First, hydraulic conductivity and aquifer thickness are inversely related, with $k \propto f^2$ and $D \propto f^{-1}$. Moreover, an upper limit on D is given by the difference between topography and the aquifer bottom. The lower bound on D is given by aquifer thickness D < ~50 cm which is considered shallow subsurface flow, and implies a stream with zero recession. Thus, fixing the value of f should yield an aquifer thickness within those limits. Based on this reasoning, the calculated hydrodynamic parameters in Fig. 5 and Table S3 were obtained for $f = 10^{-6}$. This results in younger watersheds draining fast (high k) and having shorter aquifer thicknesses (small D) than older ones for any given value of specific yield. It is probable that f does not remain constant with weathering, and likely decreases based on the observed evolution of watersheds in basaltic terrains (Ingebritsen and Scholl, 1993; Jefferson et al., 2006; Smith, 2004). But given that $k \propto f^2$, this progression will only accentuate the differences in k and D between older and younger watersheds. A decrease in f with age implies that the 3-order magnitude difference in the mean k between the watersheds with mean substrate age > 30 kyr (~2.6×10^{-4} m/s) and those with mean substrate age < 30 kyr (~1.1×10^{-1} m/s) is a minimum estimate. In Fig. 6 we have plotted D against k for a range of specific yield values $10^{-7} \leq f \leq 10^{-5}$ as uncertainty estimates. This means that in the most extreme case, with $f = 10^{-5}$ for the younger watersheds and $f = 10^{-7}$ in the older watersheds, the hydraulic conductivity k would decrease by 7 orders of magnitude between both groups. It is unlikely that specific yield will increase with weathering, compared to other processes like earthquakes or extreme rainfall events (Vittecoq et al., 2020). Given the inverse relation between specific yield f and aquifer thickness D, an increase in f results in smaller aquifer thickness that can be considered unrealistic.

Establishing a relation between the estimated hydraulic conductivities from RFA and rainfall/water infiltration rates is not straightforward. The calculated hydraulic conductivities are for a horizontally bounded aquifer, and thus our results from recession flow analyses are pertinent to horizontal groundwater flow. The anisotropy ratio for hydraulic conductivity (k_x horizontal and k_y vertical) is usually ≈ 10 to 100 for sandstones and unconsolidated materials (Singhal and Gupta, 2010); however, some studies have pointed out that the discrepancy between k_x and k_y can be much larger in volcanic regions (Ingebritsen and Scholl, 1993; Smith, 2004). This seems to be a plausible explanation for the relatively large hydraulic conductivity values obtained from RFA. Indeed, vertical fractures in basalts are a common feature and we assume these are the major pathways for rainfall infiltration (Fletcher et al., 2006; Sowards et al., 2018); but horizontal layering in lava flows, fractures, and more dramatically, the existence of lava tubes (Allred and Allred, 1997; Lau and Mink, 2006) can contribute to increase the degree of anisotropy in k.

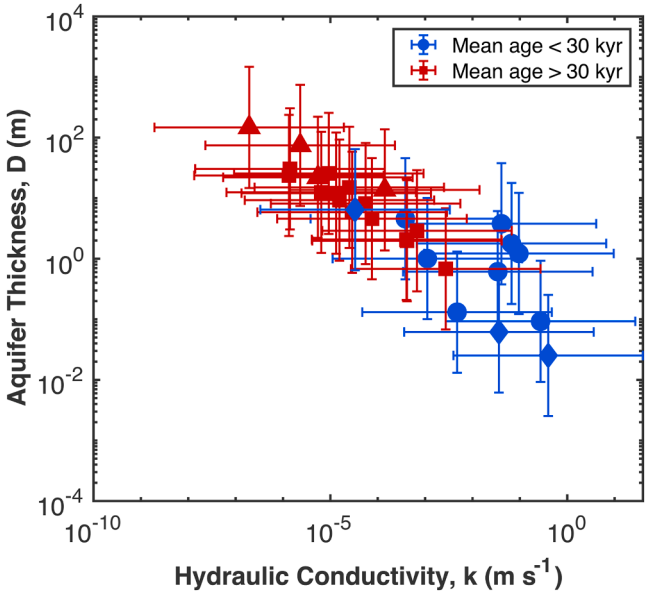

Fig. 6. Calculated hydraulic conductivity and aquifer thickness from recession flow analysis transition point (i) at center-value specific yield $f = 10^{-6}$. The error bars represent a 1-order of magnitude change in specific yield ($10^{-7} \geq f \leq 10^{-5}$). The blue symbols represent watersheds with mean bedrock age < 30 kyr both on Mauna Loa (circles) and Hualalai (diamonds). The red symbols correspond to watersheds with mean bedrock age > 30 kyr on both Mauna Kea (triangles) and Kohala (squares).

3.2. *Ephemeral streams (zero baseflow) and their recession behavior in relation to weathering history*

In the section above, we have established that hydraulic conductivity of watersheds in the Island of Hawai'i changes as a function of their weathering history for perennial streams based on recession flow analysis. While it is impossible to estimate hydraulic conductivity in ephemeral streams developed on younger substrates with zero baseflow, we can examine their recession behavior after storm events. Here we calculated the recession constant for two ephemeral streams with baseflow index BFI = 0 on the Mauna Loa lava flows in the Hilo region to compare their runoff response to discrete rainfall events. The hypothesis

behind this analysis is that for ephemeral streams with baseflow equal zero, most of the rainfall can infiltrate directly to the groundwater system and then discharge directly to the ocean (Johnson et al., 2008; Rad et al., 2007; Schopka and Derry, 2012), as shown by their null response to small rainfall events. However, in ephemeral streams runoff can be generated depending on the magnitude of the rainfall events, and their recession response will depend on the hydrodynamic properties of each watershed.

Based on the available sub-daily discharge and rainfall data we compared the recession for two contiguous ephemeral streams in the Hilo Region developed over younger rock substrates on eastern Mauna Loa (Fig. 4). The Alenaio and Waiakea streams show different recession behavior for all events during water-year 2005 (Fig. S8 and Table S4). For this analysis we focused on two events in February and September of 2005 because both were preceded by 30-days without rainfall. The February rainfall event lasts only a few hours, and the recession time to zero flow in Alenaio Stream is ~12 hours, while discharge in the older Waiakea Stream is more persistent, lasting > 48 hours before dropping to zero (Fig. 7). Their recession constants differ by an order of magnitude with $\alpha_{Alenaio}/\alpha_{Waiakea} = 10.12$. The wetter and longer storm event in September 2005 lasts over two days, and both streams flow for longer intervals. However, similarly to the recession response to the previous event, Alenaio dries up faster than Waiakea, with a ratio between the recession constants: $\alpha_{Alenaio}/\alpha_{Waiakea} = 7.66$ (Fig. 7). While the absolute values of the empirical recession constants are slightly different for the two events, they differ by the same order of magnitude despite the different forcings. These results are consistent with the the hypothesis that increasing substrate age—and thus weathering extent—among relatively young substrates results in prolonged recession in ephemeral streams, and with further exposure to weathering this can lead to the establishment of permanent flow.

The weathering history plays a major control in the recession behavior of ephemeral and perennial streams in Hawai'i. Although the analysis of ephemeral streams did not allow us to establish a direct comparable hydrodynamic metric such as hydraulic conductivity, we were able to compare the recession behavior for two ephemeral streams with different weathering history based on soil development on volcanic deposits of different age. The area weighted age for Alenaio and Waiakea streams is 2,600 and 3,000 years based on the age range of exposed volcanic deposits (Table S4). However, this metric can be biased as most streams on the Mauna Loa slopes are located on isolated patches of older deposits—kipukas—surrounded by more recent lava flows or ash deposits. We hypothesize that the presence of kipukas controls the recession behavior—and the hydrodynamic properties of a catchment—based on the observations from the Alenaio and Waiakea streams. The areal coverage of volcanic deposits older than 5,000 years in the Alenaio catchment is 6%; whereas the areal coverage of substrates older that 5,000 years is 22% in the Waiakea stream showing slower recession. We note that other gaged ephemeral streams on Mauna Loa are also associated with older kipukas (e.g., Hilea Gulch (16764000) and Pauauu Gulch (16770500), Fig. 1, Tables S1, S2).

Unfortunately, extrapolating this analysis to other watersheds is limited by the availability of high-frequency data for precipitation and discharge in Hawai'i, where scarcity of sub-hourly and sub-daily discharge data for ephemeral streams is a common issue. Many of the stream gages have limited periods of stream records, so we could only use records for two adjacent streams with a proximal rain gauge station. Additional precipitation and runoff data at high temporal resolution in regions of ephemeral streams would be valuable for investigating stream inception.

3.3. *Time-integrated weathering effects on drainage partitioning of volcanic rocks*

The numerical values for k or D derived here should be viewed as most useful for comparisons between watersheds. These results from the

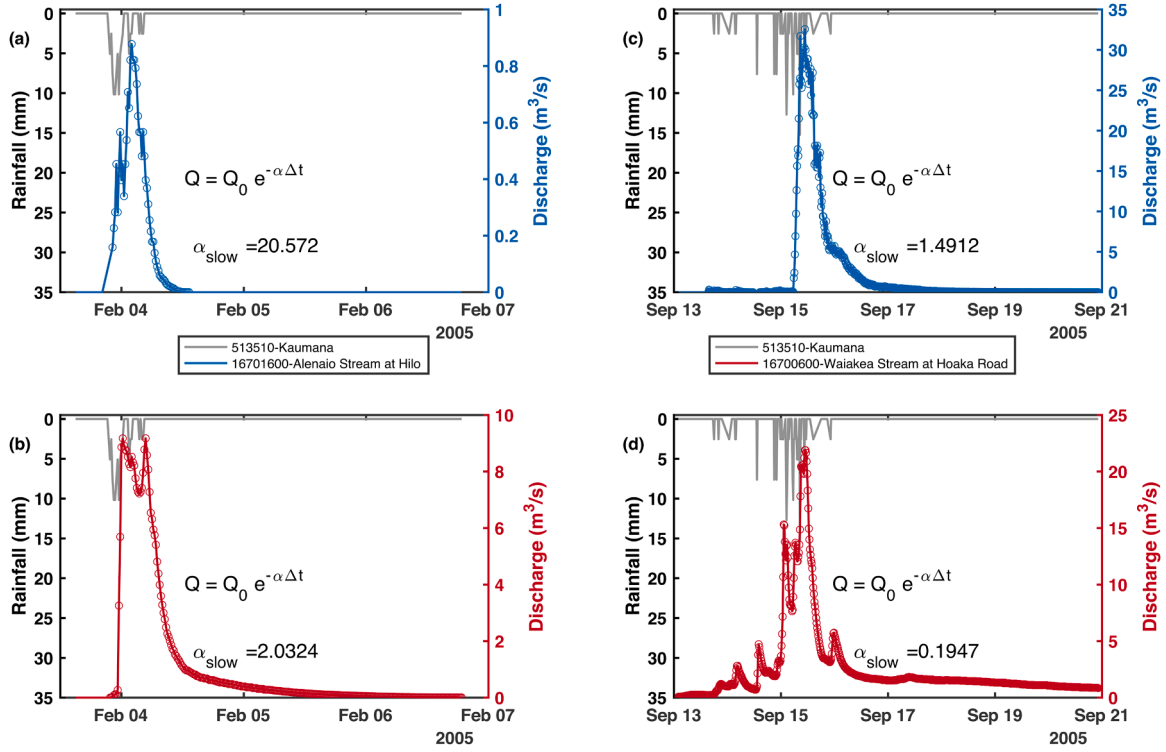

Fig. 7. Rainfall and stream discharge for two rainfall events in two contiguous watersheds. The gray curves show instantaneous (15-min intervals) rainfall for two rainfall events in February 2005 (a-b) and September 2005 (c-d). Discharge for the Alenaio Stream is shown in blue (panels a and c). Discharge for the Waiakea Stream is shown in red (panels b and d). The recession constants (α_{slow}) are calculated for the discharge data points following the last rainfall input. The circles represent the sub-daily (15–30 minutes) stream discharge values > 0.

recession flow analyses show that watershed-scale hydraulic conductivity decreases with weathering history across landscapes of increasing age on the Island of Hawai'i. Correspondingly, watershed scale aquifer thickness increases with weathering exposure, substrate age and soil development in these landscapes. Comparison of watersheds of similar age but with contrasting climates, such as the leeward (Hualalai) and windward (Mauna Loa) slopes in the younger volcanoes, supports the role of climate in addition to age as a secondary factor controlling watershed scale hydrodynamic properties. Additionally, the recession constants for two ephemeral streams covering volcanic substrates of varying age and type in Mauna Loa show the direct relationship between weathering history and hydrodynamic properties that lead to surface runoff, as the ephemeral to permanent streams with longer recessions are mostly located on small kipukas on the Mauna Loa slopes. These kipukas mostly have age ranges of 5,000 years (Sherrod et al., 2021), being significantly older and more weathered than most other substrates on Mauna Loa volcano.

Our results are consistent with other studies on basaltic terrains in volcanic islands such as Mayotte (Vittecoq et al., 2014) and Martinique (Vittecoq et al., 2023) where hydraulic conductivity decreases as a function of age. They are also consistent with observations in the Cascades (Jefferson et al., 2010; Luo et al., 2010) and Japan (Yoshida and Troch, 2016) showing increasing drainage density—and total runoff compared to groundwater partitioning—as a function of catchment substrate age. Although the watersheds in Hawai'i have younger lava flows and tephra deposits compared to those in the aforementioned locations, the fast-weathering rates on Hawai'i (Chadwick et al., 1999; Goodfellow et al., 2014; Perez-Fodich and Derry, 2019) lead to similar outcomes at shorter time scales. However, both Jefferson et al. (2010) and Yoshida and Troch (2016) found that baseflow decreased with catchment age, which differs from the observations in Hawai'i. This different behavior stems from the fact that direct groundwater discharge to the ocean is a large component of the Hawai'i water budget (e.g., Engott, 2011; Izuka et al., 2018; Johnson et al., 2008), with only a small portion of the rainfall infiltrating to the groundwater being captured downstream by surface runoff in the youngest catchments (Schopka and Derry, 2012). This is an important difference with the studied settings in the Cascades and Japan (Jefferson et al., 2010; Yoshida and Troch, 2016). In Hawai'i, An extreme example is that ephemeral streams such as Aleanio, where runoff is zero—where all discharge is via groundwater directly to the ocean—except when precipitation intensity or accumulated rainfall can temporarily outpace storage capacity. Groundwater can eventually contribute significantly baseflow in both Japan and the Cascades where the transit distances to the ocean are long and the geologic settings are more complex due to the subduction zone. In those older catchments the baseflow component decreases as hydraulic conductivity decreases. But in Hawai'i, as hydraulic conductivity decreases, the baseflow component can still increase due to progressive incision of streams with age which allows groundwater to intercept the topography, allowing emerging springs over time (Schopka and Derry, 2012).

For the sites developed on the younger volcanoes the modeled aquifer thickness was smaller ($D < 0.1$ m) in the drier and less weathered watersheds on the SW coast of Mauna Loa and Hualalai. We hypothesize that these young and drier watersheds have not developed enough to form an aquifer with significant storage capacity or correspond to deeper perched or basal aquifers. $D < 0.1$ m in these watersheds implies fast recessions, behaving as ephemeral streams. For the older watersheds, we could not find systematic differences between k and D in the watersheds in Kohala and Mauna Kea, despite both differences in substrate age (up to $> 50,000$ years) and rainfall (ΔMAP up to 200 cm/yr). Several factors might explain the lack of resolvable differences between the older and wetter watersheds in Kohala and Mauna Kea, including erosion and flank collapse (Lamb et al., 2007; Murphy et al., 2016) in the coast of eastern Kohala that may obscure the effect of weathering on hydraulic conductivity. However, changes in weathering extent in Hawai'i are manifested in the development of elemental depletion profiles and the thickness of regolith with time (Chadwick et al., 2022). The LSAG age gradient (Vitousek et al., 1997) are a series of well-studied sites across the Hawaiian Islands ranging in substrate age from 0.3 ka to 4100 kyr, at a constant MAP of 250 cm/yr. Sites on 0.3 and 2.1 kyr substrates on Kilauea show minor elemental depletion and mass loss, and they are in areas free of incision or runoff. In contrast, a site on windward Mauna Kea has a substrate age of 20-30 kyr and shows substantial elemental depletion, with >90% losses of base cations and SiO_2, and up to 50% loss of Al. Stream inception is well under way in this sector (Laupahoehoe) (Fig. 1). Older sites in Hawai'i show increasing regolith thickness, but since base cations and Si losses are already extensive by 25 kyr, regolith depletion within those older regoliths is not markedly different from the 20-30 kyr site (Goodfellow et al., 2014; Grant et al., 2022; Nelson et al., 2020; Porder et al., 2007). Additionally, climosequences of different substrate ages across the Hawaiian archipelago (Bateman et al., 2019; Chadwick et al., 2022; Goodfellow et al., 2014; Porder et al., 2007) have shown that once rainfall exceeds evapotranspiration (150 cm/yr), chemical weathering proceeds rapidly regardless of the substrate age. If, as we hypothesize, decreasing watershed scale hydraulic conductivity results from the development of a significantly weathered surface, and weathering results from a certain threshold cumulative effect of water passing through the vadose zone. Then, we would expect differences in k to be much greater among locations younger than 30 kyr, but this age-related difference in hydraulic conductivity among locations older than 30 kyr should be less evident. Similarly, deviations in k among wetter locations should also be less perceptible. Therefore, the non-linear nature or threshold effects of weathering in regolith development across Hawai'i (Chadwick and Chorover, 2001; Chadwick et al., 2022) can also be observed for both k and D, as a function of the weathering history.

From the discussion above, we propose that for the Island of Hawai'i, the landscape evolution and runoff-to-groundwater partitioning follows as: (1) Sites with substrates ages younger than 30 kyr have high initial hydraulic conductivity due to the fractured and porous nature of the lava and tephra deposits. Here, rainfall infiltrates to the groundwater, discharging directly to the basal aquifer or the ocean, and thus, ephemeral surface runoff is generated only during high rainfall events that surpass infiltration rates and storage capacity. (2) With increasing substrate age and weathering, infiltration rates decrease as watershed hydraulic conductivity is reduced, which allows runoff generation. (3) The development of stream channels promotes incision, which enables the capture of shallow groundwater—that otherwise will discharge to deeper basal aquifers or to the ocean. After further decreases in hydraulic conductivity and increased dissection, more of the groundwater intersects the surface as sub-surface quickflow and perennial streams emerge. (4) After the initiation of perennial discharge, hydraulic conductivity continues to decrease leading to increasing runoff-to-groundwater ratios. Stream formation and runoff to groundwater partitioning follows a similar evolution to that proposed by Violette et al. (2014), but at shorter timescales given the intense chemical weathering regime.

4. Conclusions

We studied 29 perennial catchments and 2 ephemeral streams in the Island of Hawai'i draining basaltic volcanic deposits of different ages. We modeled watershed-scale hydrodynamic properties on 22 of the perennial catchments based on recession flow analysis, obtaining estimates for hydraulic conductivity k and aquifer thickness D. Average saturated hydraulic conductivity decreased with weathering age up to 3 orders of magnitude; inversely, aquifer thickness increased as a function of weathering due to older bedrock substrates. The estimated aquifer thickness for two of the young watersheds is less than 10 cm, to which we attribute no aquifer storage development in these weakly weathered sites. For two catchments consisting of ephemeral streams with zero baseflow, we studied the recession response to stormflow events that

generated surface runoff; and calculated the recession constants for a short (hours) and a long-lived (days) rainfall event. While we could not extend this analysis to other paired catchments given the limited dataset, the recession constant decreases by one order of magnitude when the areal coverage of older materials (> 5,000 years) increased from 6 to 22%. Our results agree with the landscape evolution sequence observed in other basaltic terrains including volcanic islands and arc settings, where hydraulic conductivity is reduced over the weathering history of the surface. The timescale for changing the hydrodynamic properties of catchments in Hawai'i are much shorter—by 1 or 2 orders of magnitude—than in other regions given the high weathering rates.

CRediT authorship contribution statement

Alida Perez-Fodich: Writing – review & editing, Writing – original draft, Visualization, Validation, Software, Methodology, Investigation, Formal analysis, Data curation, Conceptualization. **Louis A. Derry:** Writing – review & editing, Supervision, Funding acquisition, Conceptualization. **Jean Marçais:** Writing – review & editing, Software, Methodology, Formal analysis. **M. Todd Walter:** Writing – review & editing, Methodology, Conceptualization.

Declaration of competing interest

The authors declare that they have no known competing financial interests or personal relationships that could have appeared to influence the work reported in this paper.

Data availability

All data is available from public online sources. We have provided the links to the respective data repositories used in this paper.

Acknowledgments and data availability statement

We appreciate the suggestions raised by two anonymous reviewers and the Associate Editor (Andrew Jacobson) for expedite handling of our manuscript. We would like to thank Matthew Lucas and Tom Giambelluca from the U. of Hawai'i in Manoa for their assistance with hard-to-find high-frequency precipitation data in the Big Island. Part of this research was funded by the ANR's "Make Our Planet Great Again" short-stay program to A.P.F. L.A.D acknowledges ANR Program "Investissements d'avenir" ANR-17-MPGA-0009 and U.S. NSF grants EAR 1349269 and EAR 1660923. A.P.F also acknowledges support through Fondecyt 11200656, U-Inicia UI-006/20, and Anillo ATE220029.

All stream discharge data of the studied watersheds is accessible through the U.S. Geological Survey National Water Information System NWIS on internet (Water Data for the Nation), accessed May 10, 2019, at URL http://waterdata.usgs.gov/nwis/. We used the National Hydrography Dataset (NHD) available at https://www.usgs.gov/national-hydrography/ and the Watershed Boundary Dataset (WBD) https://www.usgs.gov/national-hydrography/watershed-boundary-dataset/ for the shapefiles of the water drainage networks and watersheds. The precipitation data is accessible through National Oceanographic and Atmospheric Administration's National Center for Environmental Information (NCEI) data available on internet, accessed September 2, 2019, at https://www.ncdc.noaa.gov/cdo-web/. Mean annual rainfall map is from the Rainfall Atlas of Hawai'i (Giambelluca et al., 2013) accessible online at http://rainfall.geography.hawaii.edu/. We used the U.S. Geological Survey's geological map shapefiles of the Island of Hawai'i by Sherrod et al. (2021) at https://www.sciencebase.gov/catalog/item/60df56d5d34ed15aa3b8a39c/. The Hawai'i soil characteristics data is from the U.S. Department of Agriculture Web Soil Survey at https://websoilsurvey.sc.egov.usda.gov/App/HomePage.htm. The elevation data for the Island of Hawai'i DEM is from the SRTM 30 DEM (Becker et al., 2009). We used Peter Kovesi's Matlab package (ColorCET) for perceptually uniform maps (https://peterkovesi.com/projects/colourmaps/), and Cynthia Brewer's ColorBrewer v2.0 (http://www.ColorBrewer.org/) for colorblind- proof palettes used in all figures.

Supplementary materials

Supplementary material associated with this article can be found, in the online version, at doi:10.1016/j.epsl.2024.118687.

References

Adelinet, M., Fortin, J., D'Ozouville, N., Violette, S., 2008. The relationship between hydrodynamic properties and weathering of soils derived from volcanic rocks, Galapagos Islands (Ecuador). Environ. Geol. 56, 45–58.
Allred, K., Allred, C., 1997. Development and Morphology of Kazumura Cave, Hawaii. J. Cave Karst Stud. 59, 67–80.
Bateman, J.B., Chadwick, O.A., Vitousek, P.M., 2019. Quantitative analysis of pedogenic thresholds and domains in volcanic soils. Ecosystems. 22, 1633–1649.
Becker, J.J., Sandwell, D.T., Smith, W.H.F., Braud, J., Binder, B., Depner, J., Fabre, D., Factor, J., Ingalls, S., Kim, S.H., Ladner, R., Marks, K., Nelson, S., Pharaoh, A., Trimmer, R., Von Rosenberg, J., Wallace, G., Weatherall, P., 2009. Global bathymetry and elevation data at 30 arc seconds resolution: SRTM30_PLUS. Mar. Geod. 32, 355–371.
Boussinesq, J., 1877. Essai Sur La Théorie Des Eaux Courantes. Imprimerie Nationale, Paris, France.
Brantley, S.L., Megonigal, J.P., Scatena, F.N., Balogh-Brunstad, Z., Barnes, R.T., Bruns, M.A., Van Cappellen, P., Dontsova, K., Hartnett, H.E., Hartshorn, A.S., Heimsath, A., Herndon, E., Jin, L., Keller, C.K., Leake, J.R., McDowell, W.H., Meinzer, F.C., Mozdzer, T.J., Petsch, S., Pett-Ridge, J., Pregitzer, K.S., Raymond, P. A., Riebe, C.S., Shumaker, K., Sutton-Grier, A., Walter, R., Yoo, K., 2011. Twelve testable hypotheses on the geobiology of weathering. Geobiology. 9, 140–165.
Brutsaert, W., Lopez, J.P., 1998. Basin-scale geohydrologic drought flow features of riparian aquifers in the southern Great Plains. Water. Resour. Res. 34, 233–240.
Brutsaert, W., Nieber, J.L., 1977. Regionalized drought flow hydrographs froma a mature glaciated plateau. Water. Resour. Res. 13, 637–644.
Chadwick, O.A., Chorover, J., 2001. The chemistry of pedogenic thresholds. Geoderma 100, 321–353.
Chadwick, O.A., Chorover, J., Chadwick, K.D., Bateman, J.B., Slessarev, E.W., Kramer, M., Thompson, A., Vitousek, P.M., 2022. Constraints of climate and age on soil development in Hawai'i. In: Wymore, A.S., Yang, W.H., Silver, W.L., McDowell, W.H., Chorover, J. (Eds.), Biogeochemistry of the Critical Zone. Springer International Publishing, Cham, pp. 49–88.
Chadwick, O.A., Derry, L.A., Vitousek, P.M., Huebert, B.J., Hedin, L.O., 1999. Changing sources of nutrients during four million years of ecosystem development. Nature 397, 491–497.
Chadwick, O.A., Gavenda, R.T., Kelly, E.F., Ziegler, K., Olson, C.G., Elliott, W.C., Hendricks, D.M., 2003. The impact of climate on the biogeochemical functioning of volcanic soils. Chem. Geol. 202, 195–223.
Curtis, J.A., Burns, E.R., Sando, R., 2020. Regional patterns in hydrologic response, a new three-component metric for hydrograph analysis and implications for ecohydrology, Northwest Volcanic Aquifer Study Area, USA. J. Hydrol.-Regional Stud. 30.
Custodio, E., 2004. Hydrogeology of volcanic rocks. In: Kovalevsky, V.S., Kruseman, G. P., Rushton, K.R. (Eds.), Groundwater studies: An international guide for hydrogeological investigations. UNESCO, Paris, p. 423.
Deolankar, S.B., 1980. The Deccan Basalts of Maharashtra, India — Their potential as aquifers. Ground Water 18, 434–437.
Engott, J.A., 2011. A water-budget model and assessment of groundwater recharge for the Island of Hawai'i., Scientific Investigations Report. U. S. Geological Survey, p. 53.
Fletcher, R.C., Buss, H.L., Brantley, S.L., 2006. A spheroidal weathering model coupling porewater chemistry to soil thicknesses during steady-state denudation. Earth. Planet. Sci. Lett. 244, 444–457.
Fortini, L.B., Leopold, C.R., Perkins, K.S., Chadwick, O.A., Yelenik, S.G., Jacobi, J.D., Bishaw, K., Gregg, M., 2021. Landscape level effects of invasive plants and animals on water infiltration through Hawaiian tropical forests. Biol. Invasions. 23, 2155–2172.
Giambelluca, T.W., Chen, Q., Frazier, A.G., Price, J.P., Chen, Y.L., Chu, P.S., Eischeid, J. K., Delparte, D.M., 2013. ONLINE RAINFALL ATLAS OF HAWAI'I. Bull. Amer. Meteorol. Soc. 94, 313–316.
Goodfellow, B.W., Chadwick, O.A., Hilley, G.E., 2014. Depth and character of rock weathering across a basaltic-hosted climosequence on Hawai` i. Earth Surf. Process. Landf. 39, 381–398.
Grant, K.E., Galy, V.V., Haghipour, N., Eglinton, T.I., Derry, L.A., 2022. Persistence of old soil carbon under changing climate: the role of mineral-organic matter interactions. Chem. Geol. 587.
Horton, R.E., 1933. The role of infiltration in the hydrologic cycle. Trans.-Amer. Geophys. Union 14, 446–460.
Huang, C.C., Yeh, H.F., 2019. Hydrogeological Parameter Determination in the Southern Catchments of Taiwan by Flow Recession Method. Water. (Basel) 11, 16.

Ingebritsen, S.E., Scholl, M.A., 1993. The hydrogeology of Kilauea volcano. Geothermics. 22, 255–270.
Izuka, S.K., 2011. Scientific Investigations Report.
Izuka, S.K., Engott, J.A., Rotzoll, K., Bassiouni, M., Johnson, A.G., Miller, L.D., Mair, A., 2018. Volcanic aquifers of Hawai'i—Hydrogeology, water budgets, and conceptual models, Scientific Investigations Report, Version 1.0: June 13, 2016; Version 2.0: March 1, 2018 ed, Reston, VA, p. 172.
Jefferson, A., Grant, G., Rose, T., 2006. Influence of volcanic history on groundwater patterns on the west slope of the Oregon High Cascades. Water. Resour. Res. 42, 15.
Jefferson, A., Grant, G.E., Lewis, S.L., Lancaster, S.T., 2010. Coevolution of hydrology and topography on a basalt landscape in the Oregon Cascade Range, USA. Earth Surf. Process. Landf. 35, 803–816.
Johnson, A.G., Glenn, C.R., Burnett, W.C., Peterson, R.N., Lucey, P.G., 2008. Aerial infrared imaging reveals large nutrient-rich groundwater inputs to the ocean. Geophys. Res. Lett. 35, 6.
Kirchner, J.W., 2009. Catchments as simple dynamical systems: catchment characterization, rainfall-runoff modeling, and doing hydrology backward. Water. Resour. Res. 45.
Lamb, M.P., Howard, A.D., Dietrich, W.E., Perron, J.T., 2007. Formation of amphitheater-headed valleys by waterfall erosion after large-scale slumping on Hawai'i. Geol. Soc. Am. Bull. 119, 805–822.
Lau, L.S., Mink, J.F., 2006. Hydrology of the Hawaiian Islands. University of Hawai'i Press, Honolulu.
Lohse, K.A., Dietrich, W.E., 2005. Contrasting effects of soil development on hydrological properties and flow paths. Water. Resour. Res. 41. W12419-W12419.
Luo, W., Grudzinski, B.P., Pederson, D., 2010. Estimating hydraulic conductivity from drainage patterns-A case study in the Oregon Cascades. Geology. 38, 335–338.
Malvicini, C.F., Steenhuis, T.S., Walter, M.T., Parlange, J.Y., Walter, M.F., 2005. Evaluation of spring flow in the uplands of Matalom, Leyte, Philippines. Adv. Water Resour. 28, 1083–1090.
Mendoza, G.F., Steenhuis, T.S., Walter, M.T., Parlange, J.Y., 2003. Estimating basin-wide hydraulic parameters of a semi-arid mountainous watershed by recession-flow analysis. J. Hydrol. 279, 57–69.
Montgomery, D.R., Dietrich, W.E., 1988. Where do channels begin. Nature 336, 232–234.
Murphy, B.P., Johnson, J.P.L., Gasparini, N.M., Sklar, L.S., 2016. Chemical weathering as a mechanism for the climatic control of bedrock river incision. Nature 532, 223-+.
Mushiake, K., Takahashi, Y., Ando, Y., 1981. Effects of basin geology on river-flow regime in mountainous areas of Japan. In: Proceedings of the Japan Society of Civil Engineers 1981, pp. 51–62.
Nelson, S.T., Barton, B., Burnett, M.W., McBride, J.H., Brown, L., Spring, I., 2020. The lateral and vertical growth of laterite weathering profiles, Hawaiian Islands, USA. Earth Surf. Process. Landf 45, 2940–2953.
Oyarzun, R., Godoy, R., Nunez, J., Fairley, J.P., Oyarzun, J., Maturana, H., Freixas, G., 2014. Recession flow analysis as a suitable tool for hydrogeological parameter determination in steep, arid basins. J. Arid. Environ. 105, 1–11.
Parlange, J.Y., Stagnitti, F., Heilig, A., Szilagyi, J., Parlange, M.B., Steenhuis, T.S., Hogarth, W.L., Barry, D.A., Li, L., 2001. Sudden drawdown and drainage of a horizontal aquifer. Water. Resour. Res. 37, 2097–2101.
Perez-Fodich, A., Derry, L.A., 2019. Organic acids and high soil CO2 drive intense chemical weathering of Hawaiian basalts: Insights from reactive transport models. Geochim. Cosmochim. Acta 249, 173–198.
Porder, S., Hilley, G.E., Chadwick, O.A., 2007. Chemical weathering, mass loss, and dust inputs across a climate by time matrix in the Hawaiian Islands. Earth. Planet. Sci. Lett. 258, 414–427.
Rad, S.D., Allegre, C.J., Louvat, P., 2007. Hidden erosion on volcanic islands. Earth. Planet. Sci. Lett. 262, 109–124.
Rempe, D.M., Dietrich, W.E., 2014. A bottom-up control on fresh-bedrock topography under landscapes. Proc. Natl. Acad. Sci. U. S. A. 111, 6576–6581.
Riebe, C.S., Hahm, W.J., Brantley, S.L., 2017. Controls on deep critical zone architecture: a historical review and four testable hypotheses. Earth Surf. Process. Landf. 42, 128–156.
Roques, C., Rupp, D.E., Selker, J.S., 2017. Improved streamflow recession parameter estimation with attention to calculation of - dQ/dt. Adv. Water Resour. 108, 29–43.
Rotzoll, K., El-Kadi, A.I., 2008. Estimating hydraulic conductivity from specific capacity for Hawaii aquifers. USA. Hydrogeol. J. 16, 969–979.
Rupp, D.E., Selker, J.S., 2006. Information, artifacts, and noise in dQ/dt-Q recession analysis. Adv. Water Resour. 29, 154–160.
Sanchez-Murillo, R., Brooks, E.S., Elliot, W.J., Gazel, E., Boll, J., 2015. Baseflow recession analysis in the inland Pacific Northwest of the United States. Hydrogeol. J. 23, 287–303.
Schopka, H.H., Derry, L.A., 2012. Chemical weathering fluxes from volcanic islands and the importance of groundwater: The Hawaiian example. Earth. Planet. Sci. Lett. 339, 67–78.
Sherrod, D.R., Sinton, J.M., Watkins, S.E., Brunt, K.M., 2021. Geologic map of the State of Hawaii. Scientific Investigations Map, Reston, VA, p. 72.
Singhal, B.B.S., Gupta, R.P., 2010. Applied Hydrogeology of Fractured Rocks Second Edition Introduction and Basic Concepts, Applied Hydrogeology of Fractured Rocks, Second Edition. Springer, Dordrecht, 1-+.
Smith, R.P., 2004. Geologic setting of the Snake River Plain aquifer and vadose zone. Vadose Zone J. 3, 47–58.
Sowards, K.F., Nelson, S.T., McBride, J.H., Bickmore, B.R., Heizler, M.T., Tingey, D.D., Rey, K.A., Yaede, J.R., 2018. A conceptual model for the rapid weathering of tropical ocean islands: a synthesis of geochemistry and geophysics, Kohala Peninsula, Hawaii, USA. Geosphere 14, 1324–1342.
Troch, P.A., Detroch, F.P., Brutsaert, W., 1993. Effective water-table depth to describe initial conditions prior to storm rainfall in humid regions. Water. Resour. Res. 29, 427–434.
Vannier, O., Braud, I., Anquetin, S., 2014. Regional estimation of catchment-scale soil properties by means of streamflow recession analysis for use in distributed hydrological models. Hydrol. Process. 28, 6276–6291.
Violette, S., d'Ozouville, N., Pryet, A., Deffontaines, B., Fortin, J., Adelinet, M., 2014. Hydrogeology of the Galápagos Archipelago. Galápagos 167–183.
Vitousek, P., 2004. Nutrient cycling and limitation: Hawai'i as a model system. Nutrient cycling and limitation: Hawai'i as a model system 1–223 i-xx.
Vitousek, P.M., Chadwick, O.A., Crews, T.E., Fownes, J.H., Hendricks, D.M., Herbert, D. A., 1997. Soil and ecosystem development across the Hawaiian islands. GSa Today 7, 1–8.
Vittecoq, B., Deparis, J., Violette, S., Jaouën, T., Lacquement, F., 2014. Influence of successive phases of volcanic construction and erosion on Mayotte Island's hydrogeological functioning as determined from a helicopter-borne resistivity survey correlated with borehole geological and permeability data. J. Hydrol. 509, 519–538.
Vittecoq, B., Fortin, J., Maury, J., Violette, S., 2020. Earthquakes and extreme rainfall induce long term permeability enhancement of volcanic island hydrogeological systems. Sci. Rep. 10.
Vittecoq, B., Reninger, P.A., Bellier, V., Taïlamé, A.L., Nacimento, L., Gros, E., Violette, S., 2023. Montagne Pelee volcano (Martinique, in the French Lesser Antilles) hydrogeological system revealed by high-resolution helicopter-borne electromagnetic imagery. Hydrogeol. J. 31, 1331–1352.
Vogel, R.M., Kroll, C.N., 1992. Regional geohydrologic-geomorphic relationships for the estimation of low-flow statistics. Water. Resour. Res. 28, 2451–2458.
Wolfe, E.W., Morris, J., 1996. Geologic map of the Island of Hawaii. IMAP. U.S. Geol. Surv.
Wolff, R.G., 1982. Physical properties of rocks; porosity, permeability, distribution coefficients, and dispersivity, Open-File Report, - ed.
Yoshida, T., Troch, P.A., 2016. Coevolution of volcanic catchments in Japan. Hydrol. Earth Syst. Sci. 20, 1133–1150.
Zecharias, Y.B., Brutsaert, W., 1988. Recession characteristics of groundwater outflow and base-flow from mountainous watersheds. Water. Resour. Res. 24, 1651–1658.